SUPPORTING INFORMATION

Intrinsic anomalous Hall effect in thin films of topological kagome ferromagnet Fe_3Sn_2

Kacho Imtiyaz Ali Khan,† Ram Singh Yadav,† Himanshu Bangar,† Akash Kumar,† Niru Chowdhury,† Prasanta Kumar Muduli,‡ and Pranaba Kishor Muduli*,*,†

†*Department of Physics, Indian Institute of Technology Delhi, Hauz Khas, New Delhi, 110016, India*

‡ *Department of Physics, Indian Institute of Technology Madras, Chennai, Tamil Nadu-600036, India.*

E-mail: muduli@physics.iitd.ac.in

S1: Comparison of Fe_3Sn_2 thin films with and without Ta seed layer.

In Fig S1(a), we show the GI-XRD measurements from Fe_3Sn_2 thin films with (green symbols) and without (black symbols) Ta seed layer. Both the samples show identical Bragg peaks from both FM (red) and AFM (green) phases. In Fig S1(b), VSM measurement shows that in both with and without Ta seed layer samples shows the 50% reduction of saturation magnetization M_S compared to Pt seed layer samples. Both XRD and VSM measurements indicate that the growth of Fe_3Sn_2 with and without the Ta seed layer leads to a reduction

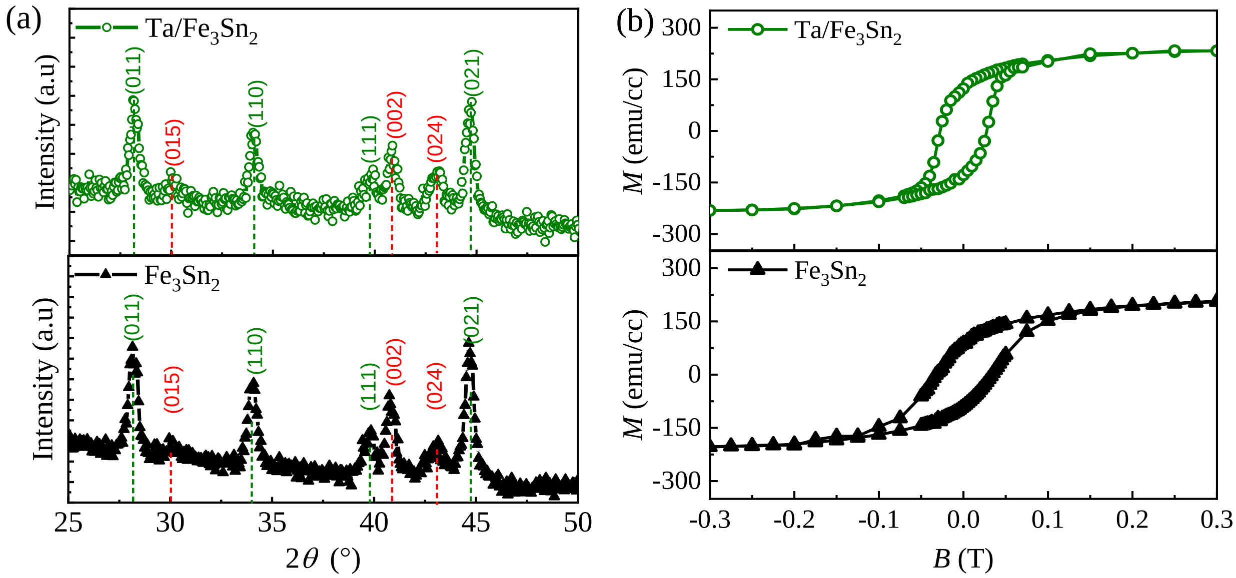

Figure S1: (a) GI-XRD pattern of Fe_3Sn_2 thin film (70 nm) deposited with (symbol: open green circle) and without (symbol: filled triangle black) Ta seed layer. (b) The room temperature magnetization curves for Fe_3Sn_2 thin film (70 nm) with and without Ta seed layer.

of M_S from bulk value due to additional formation of AFM phase along with FM phase.

S2: Atomic force microscopy analysis.

In Figure S2(a,b), we show two-dimensional AFM morphology of Fe_3Sn_2 thin films with Ta and Pt seed layer deposited on Si/SiO_2 substrate. We found that a bit larger root mean square ($r_{rms}^{Pt} \approx 3.9$ nm) roughness in Pt/Fe_3Sn_2 thin film samples could be originated from large size of FM grains. However, Ta seed layer based Fe_3Sn_2 thin film sample shows smaller ($r_{rms}^{Ta} \approx 0.5$ nm) roughness.

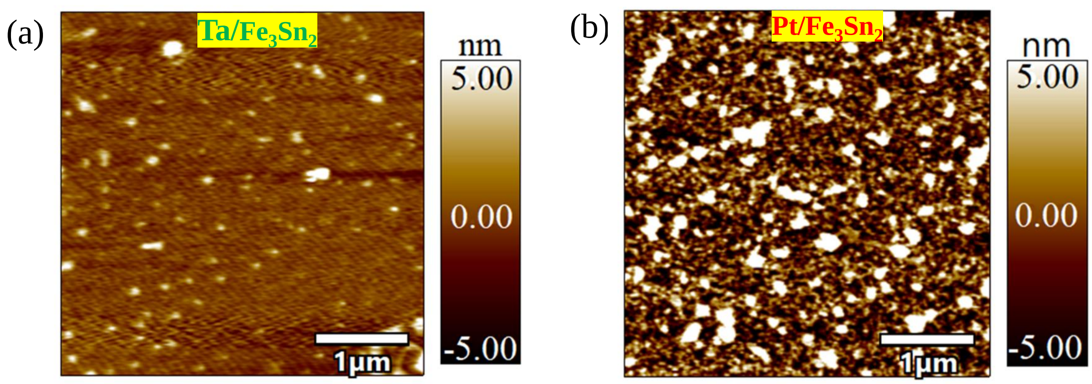

Figure S2: Atomic force microscopy images of (a) Ta/Fe_3Sn_2 and, (b) Pt/Fe_3Sn_2.

S3: Temperature dependent magnetization measurements.

In Figure S3(a, b) shows the in-plane magnetization hysteresis loop for Fe_3Sn_2 thin film at various temperatures with Ta and Pt seed layer samples. Saturation magnetization increases monotonically with the decrease in temperature, from which the M_S-T plot data shown in Fig. 4(b) of the main text is extracted. We also observed a larger coercivity field (at all measured temperatures) for Ta/Fe_3Sn_2 compared to Pt/Fe_3Sn_2 as shown in Fig S3(c). However, a smaller value of $H_C = 42.5$ mT even at 10 K for Pt/Fe_3Sn_2 sample could be an indication of less number pinning sites at the grain boundaries consistent with SEM results.

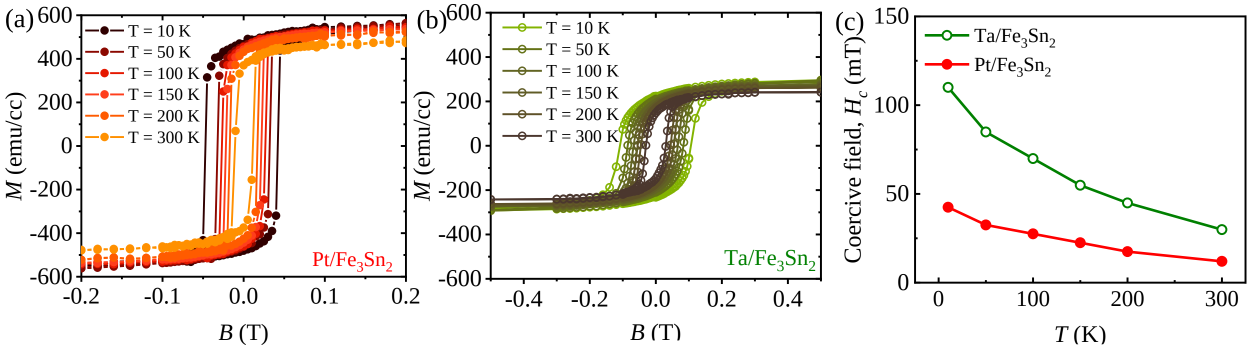

Figure S3: Temperature-dependent magnetization curves for (a) Pt/Fe_3Sn_2 and, (b) Ta/Fe_3Sn_2. (c) The behavior of coercive field H_c as a function of temperature for both the samples.

S4: Micromagnetic simulation.

In order to understand the dependence of magnetic properties in mixed-phase Ta/Fe_3Sn_2 thin films, we micromagntically simulate these polycrystalline films with different FM grain percentages created with the help of Voronoi tessellation. Based on the experimental (XRD & M-H) results, we assumed that Pt seed layer gives rise to pure FM (Fe_3Sn_2) phase, whereas Ta seed layer leads to a mixed phase of both FM and AFM phase. Therefore, we considered Pt seed layer Fe_3Sn_2 with 100%-FM (0%-AFM) grains and Ta seed layer Fe_3Sn_2 with 50%-FM (50%-AFM) grains. Here, we performed the simulation using Mumax^3[Ref. [1]] software and the material parameters of Fe_3Sn_2 were set as $A_{ex} = 14$ pJ/m and $K_u = 53$ kJ/m^3 [2–4]. We set a cuboidal geometry ($4\ \mu\text{m} \times 4\ \mu\text{m} \times 4\ \mu\text{m}$) using a mesh cell size ($8\ \text{nm} \times 8\ \text{nm} \times 8\ \text{nm}$) such that the cell size should not exceed exchange length ($l_{ex} < 8.4$ nm). Here, for simplicity, we consider the magnetization dynamics in 2D system considering one cell along the thickness. However, for a 3D system, it will be trivial to design and understand the dynamics in the polycrystalline phase of ferromagnetic domains. In this simulation, time-dependent reduced magnetization ($\vec{m} = \vec{M}/M_s$), we only incorporate Landau-Lifshitz torque term and Gilbert's damping torque ($\vec{\tau}_{LL}$) term.

$$\frac{\partial \vec{m}}{\partial t} = -\gamma\mu_0(\vec{m} \times \vec{H}_{eff}) + \alpha\left(\vec{m} \times \frac{\partial \vec{m}}{\partial t}\right) \tag{S1}$$

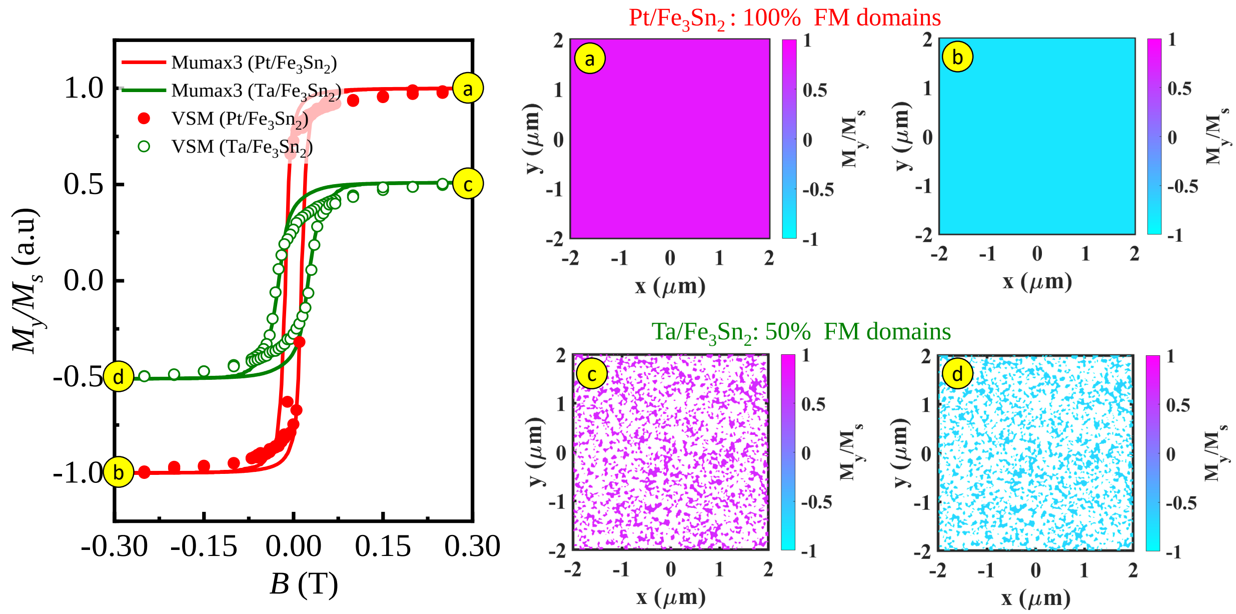

Figure S4: Micro-magnetically simulated magnetization curve for 100% FM domains (Pt/Fe_3Sn_2) and 50% FM domains (Ta/Fe_3Sn_2). On left hand side, Symbol 'a','b','c' and, 'd' shows the saturation field ($\approx \pm 3$ T) for both the cases. On right hand side, shows the snapshots of respective y component of magnetization (M_y/M_S) for both the cases at ($\approx \pm 0.3$ T).

where γ and α are the gyromagnetic ratio of electron and dimensionless damping constant, respectively.

In Fig. S4, we show simulated magnetization loops for magnetic fields of -0.3 T to +0.3 T to-gather with experimental data. Symbols show the experimental values obtained from the VSM measurement technique, whereas solid line shows the simulated values. We obtain excellent agreement of both saturation magnetization, M_S and coercivity field (H_c) by assuming that Ta/Fe_3Sn_2 has 50 % FM phase and 50% AFM (zero net magnetization) phase.

S5: Composition analysis.

Figure S5 (a, b) shows the energy dispersive X-ray (EDX) analysis spectrum for the elemental and composition analysis of Fe and Sn atoms in Fe_3Sn_2 with seed layer (Ta, Pt). The atomic and weight percent of these two elements are summarized in Table S1 for Pt/Fe_3Sn_2 and

Ta/Fe_3Sn_2 thin film, respectively.

Table S1: Element and composition analysis.

Sample	Element	Weight %	Atomic %
	Fe	41.6	60.2
Pt/Fe_3Sn_2	Sn	58.4	39.8
	Fe	43.7	62.2
Ta/Fe_3Sn_2	Sn	56.3	37.8

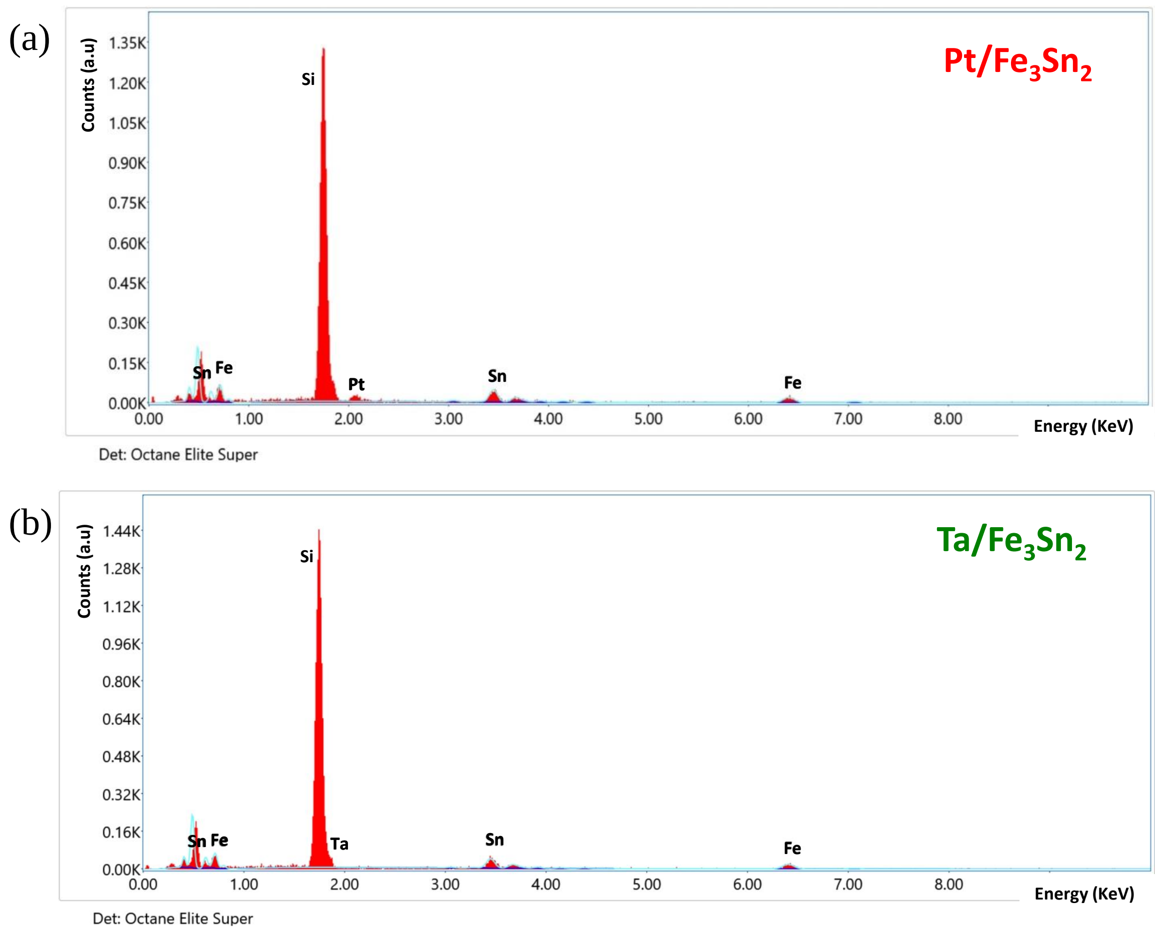

Figure S5: EDX spectrum of Fe, Sn, Pt and Ta in (a) Pt/Fe_3Sn_2 and (b) Ta/Fe_3Sn_2 thin films.

S6: Roughness improvement by combining Ta/Pt seed layer.

As discussed in supplementary section S2, the Pt seed layer results in an increase in the root mean square (RMS) roughness of the Pt/Fe_3Sn_2 thin film. However, the Pt seed layer is critical in the formation of pure ferromagnetic phase. Furthermore, we found that by using a Ta seed layer, the RMS roughness is reduced to < 1 nm. Hence, to achieve a ferromagnetic phase with low roughness, we have grown Fe_3Sn_2 thin films with a seed layer consisting of Ta(1.5 nm)/Pt(5 nm). The RMS roughness is found to be reduced with the Ta/Pt seed layer. For a 70 nm-thick film, the RMS roughness is $\sim$ 1.6 nm as shown in Fig. S6 (a). We also found a further reduction of the RMS roughness down to $\sim$ 0.4 nm for a 20 nm-thick film, as shown in Fig. S6 (b). These results demonstrate that a Ta/Pt seed layer helps in the growth of a pure ferromagnetic phase of Fe_3Sn_2 with reduced roughness.

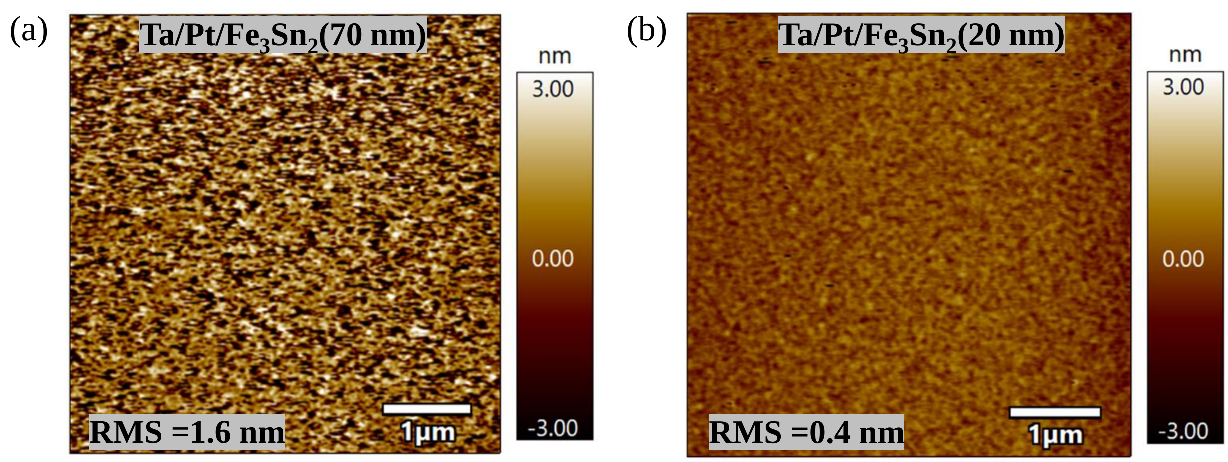

Figure S6: (a) Atomic force microscopy images for Fe_3Sn_2 thin films with Ta/Pt seed layer for a scan area of (5 μm $\times$ 5 μm) for thicknesses of (a) 70 nm and, (b) 20 nm measured at room temperature.

References

(1) Vansteenkiste, A.; Leliaert, J.; Dvornik, M.; Helsen, M.; Garcia-Sanchez, F.; Van Waeyenberge, B. The design and verification of MuMax3. *AIP Adv.* **2014**, *4*, 107133.

(2) Wang, B.; Wu, P.-k.; Bagués Salguero, N.; Zheng, Q.; Yan, J.; Randeria, M.; McComb, D. W. Stimulated Nucleation of Skyrmions in a Centrosymmetric Magnet. *ACS nano* **2021**, *15*, 13495–13503.

(3) Tang, J.; Wu, Y.; Kong, L.; Wang, W.; Chen, Y.; Wang, Y.; Soh, Y.; Xiong, Y.; Tian, M.; Du, H. Two-dimensional characterization of three-dimensional magnetic bubbles in Fe_3Sn_2 nanostructures. *Natl. Sci. Rev.* **2021**, *8*, nwaa200.

(4) Altthaler, M.; Lysne, E.; Roede, E.; Prodan, L.; Tsurkan, V.; Kassem, M. A.; Nakamura, H.; Krohns, S.; Kézsmárki, I.; Meier, D. Magnetic and geometric control of spin textures in the itinerant kagome magnet Fe_3Sn_2. *Phys. Rev. Res.* **2021**, *3*, 043191.